PHYSICAL REVIEW A VOLUME 40, NUMBER 3 AUGUST 1, 1989

Laser excitation of Stark-induced resonances

G. Alber*
Institute for Theoretical Physics, University of Innsbruck, A-6020 Innsbruck, Austria
(Received 6 February 1989)

We study laser excitation of a hydrogen atom in the presence of a static electric field in the energy region slightly above the zero-field photoionization threshold. With the help of a multiple-scattering expansion, we derive an analytic expression for the time evolution of the initial-state probability, which is nonperturbative with respect to the laser field and which is asymptotically valid in the limit of small electric fields. This allows us to study how the characteristics of the classical periodic orbit, which qualitatively has been associated with the Stark-induced resonances above the zero-field photoionization threshold, manifest themselves in the dynamics of the laser-excitation process.

I. INTRODUCTION

Recently we have developed a theory[1-3] that describes laser excitation of Rydberg states close to a photoionization threshold. It is based on the observation that the atom-laser interaction is localized in a reaction zone, which typically extends only a few Bohr radii around the atomic nucleus and is small in comparison with the extent of high-lying Rydberg states.[4] Within this theory it has been shown that photon absorption due to a short or intense laser pulse leads to the generation of a radial electronic Rydberg wave packet as long as the characteristic excitation time, which is either the pulse duration or the depletion time of the initially occupied bound state, is short in comparison with the classical orbit time of the excited electron. Until now our work has been concentrated on cases, however, where the dynamics of the generated Rydberg wave packet at large distances from the atomic nucleus is determined by the Coulomb potential of the ionic core.

A hydrogen atom placed in a homogeneous static electric field represents one of the simplest physical examples where this is no longer the case. Laboratory electric fields up to a few kV/cm, which are negligible within distances of a few Bohr radii around the atomic nucleus dominate the Coulomb field of the ionic core at large distances and may thus significantly influence Rydberg and continuum states close to the photoionization threshold.[5,6] Historically, the behavior of a hydrogen atom in a static electric field has been one of the first problems to which quantum mechanics has been applied.[7] However, certain aspects of this problem have become clear only recently. In particular, the experiments of Freeman *et al.*[8] and others,[9-11] in which asymmetric modulations of the photoabsorption cross section above the zero-field photoionization threshold have been found, have stimulated theoretical work.[12-17] These studies have concentrated on the determination of the frequency dependence of the photoabsorption cross section, which characterizes laser excitation by a weak and long laser pulse. In particular, it has been shown that these modulations can qualitatively be attributed to an unstable periodic motion of the excited electron in the direction of the applied electric field.[13,17,18] This kind of motion is even possible for energies above the zero-field photoionization threshold.

In this paper, we extend our previous work and study one-photon excitation of a hydrogen atom in the presence of a homogeneous static electric field. Our approach is not only nonperturbative with respect to the static electric field but also with respect to the laser pulse, so that we are able to describe effects due to depletion of the initially occupied bound atomic state. Motivated by the recent work on the Stark effect in hydrogen, we concentrate on the energy region slightly above the zero-field photoionization threshold, where the asymmetric modulations of the photoabsorption cross section have been found. In particular, we are interested in situations where the exciting laser pulse becomes so intense that an electronic wave packet is generated. The time evolution of this wave packet is reflected in the time dependence of the initial-state probability, because whenever the excited wave packet returns to the reaction zone, where the atom-laser interaction is localized, it may recombine with the ionic core to increase the initial-state probability.[2] This provides a method for studying the dynamics of the unstable periodic motion of the excited electron, which qualitatively has been associated with the modulations of the photoabsorption cross section above the zero-field photoionization threshold.

In Sec. II, we present the basic equations describing one-photon excitation of hydrogen in the presence of a static electric field above the zero-field photoionization threshold. The resulting time evolution of the initial-state probability is discussed in Sec. III. Taking advantage of the separability of the hydrogenic Stark problem in parabolic coordinates and using semiclassical methods together with a multiple-scattering representation of the initial-state-probability amplitude, we are able to relate this quantum-mechanical observable asymptotically to quantities, which characterize the classical motion of the excited electron under the combined influence of the Coulomb field of the ionic core and the external static electric field.

II. BASIC EQUATIONS

In this section, we discuss the basic equations describing one-photon excitation of a hydrogen atom by an intense laser pulse in the presence of a static electric field. We consider a one-photon excitation process where an intense laser pulse of field strength $\mathbf{E}=\mathcal{E}\mathbf{e}e^{-i\omega t}+\text{c.c.}$ excites a hydrogen atom from a low-lying bound state $|g\rangle$ with energy ε_g to continuum states close to the photoionization threshold. In addition, a homogeneous static electric field of field strength F is applied to the atom in the positive z direction. This static field is assumed to be weak in the sense that its influence on the initially occupied energetically low-lying bound state $|g\rangle$, which is typically localized in a spatial region of a few Bohr radii around the atomic nucleus, can be neglected, i.e., $F \ll 1$ (we use hartree atomic units). However, at large distances from the atomic nucleus of the order of $r > F^{-1/2}$ the static electric field dominates the long-range Coulomb field due to the ionic core and may thus significantly influence excited Rydberg and continuum states close to the zero-field ($F=0$) photoionization threshold.[6]

In particular, we are interested in the influence of the static electric field on the time evolution of the initial-state-probability amplitude $a_g(t)$ in a case where we are exciting states close to the photoionization threshold. Assuming an instantaneous turn-on of the exciting laser pulse at $t=0$ in the dipole and rotating-wave approximation, the Laplace transform of the initial-state-probability amplitude is given by[2]

$$a_g(z)=i[z-\varepsilon_g-\Sigma(z+\omega)]^{-1}\ , \tag{1}$$

with the resonant part of the self energy

$$\Sigma(\varepsilon)=\langle g|D^{\dagger}(\varepsilon-H_A+i0)^{-1}D|g\rangle$$

incorporating all effects due to the intense laser field. The atomic Hamiltonian H_A includes the interaction term $-\boldsymbol{\mu}\cdot\mathbf{F}$ due to the external homogeneous static electric field $\mathbf{F}=F\mathbf{e}_z$ and $D=-\boldsymbol{\mu}\cdot\mathcal{E}\mathbf{e}$ is the dipole-interaction term due to the laser field with the atomic dipole operator $\boldsymbol{\mu}$. In Eq. (1) we have neglected photon absorption from the excited states.

In order to determine the energy dependence of the self-energy, we exploit the fact that the atom-laser interaction takes place in a reaction zone, which is of the size of the initially occupied atomic state $|g\rangle$ and therefore extends only a few Bohr radii around the atomic nucleus. In this region, the external static electric field is negligible.[16] This finite range of the radiative coupling allows us to characterize the laser-excitation process by a few intensity-dependent parameters, which are approximately energy independent across the zero-field photoionization threshold and do not depend on the electric field strength as long as $F \ll 1$. The influence of the static electric field on the dynamics of the excited electron at large distances from the ionic core can be taken into account with the help of semiclassical methods.

Taking advantage of the separability of the Hamiltonian H_A in parabolic coordinates $\xi=r+z$, $\eta=r-z$ (Ref. 19), the self-energy of the initial state can be written in the form

$$\Sigma(\varepsilon)=\sum_m \int_{-\infty}^{\infty} d\varepsilon' \sum_{n_1=0}^{\infty} |\langle \varepsilon'\beta m|D|g\rangle|^2(\varepsilon-\varepsilon'+i0)^{-1}\ . \tag{2}$$

$|\varepsilon\beta m\rangle$ is an energy normalized eigenstate of H_A with energy ε, magnetic quantum number m, and separation constant β. Classically β can only assume values in the range $0\le\beta\le 1$ and is related to the angle α between the intial velocity of the electron, which is excited at $\xi=\eta=0$, and the direction of the applied static electric field by[13]

$$\beta=\cos^2(\alpha/2)\ . \tag{3}$$

In general, the Coulomb force due to the ionic core and the applied electric field leads to a periodic motion of the excited electron for all energies in the ξ coordinate, whereas its motion in the η coordinate is dominated by a potential barrier at negative energies, as schematically shown in Fig. 1. This implies that contrary to the case of a pure Coulomb field even for $\varepsilon>0$ the excited electron

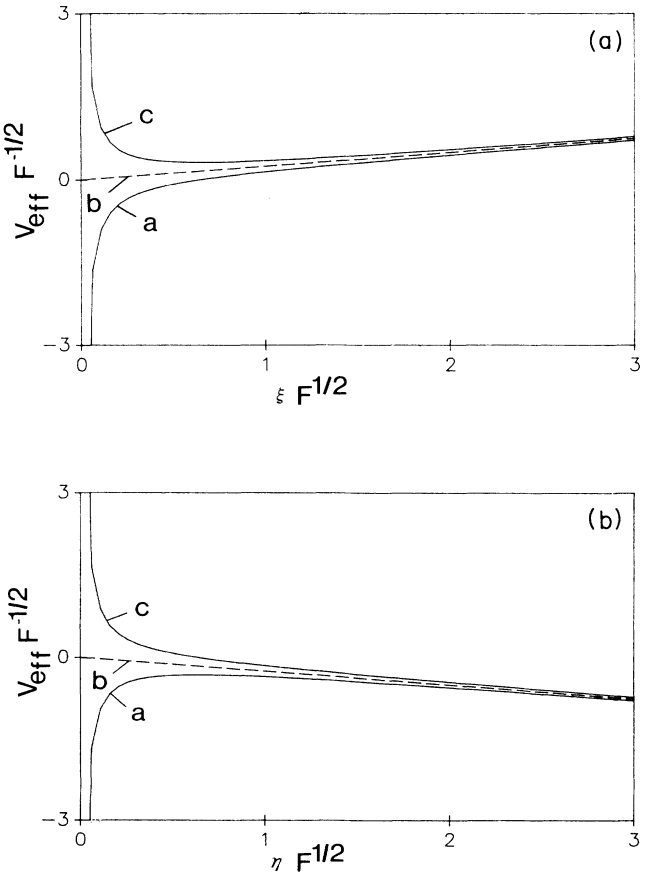

FIG. 1. Effective potentials V_{eff} of the ξ and η coordinates for $m=0$ and different values of β. Panel (a) $V_{\text{eff}}(\xi)=-\beta/\xi+0.25F\xi$; $\beta=0.1$, curve a; 0, curve b; -0.1, curve c. Panel (b) $V_{\text{eff}}=-(1-\beta)/\eta-0.25F\eta$; $\beta=0.9$, curve a; 1, curve b; 1.1, curve c.

may perform a periodic motion. The quantum number n_1, which is associated with this motion, is related to ε,β,m by the semiclassical quantization condition[16]

$$w(\varepsilon,\beta,m)=\pi(n_1+\tfrac{1}{2}) , \tag{4}$$

with the classical action

$$w(\varepsilon,\beta,m)=\int_{\xi_<}^{\xi_>} d\xi[\varepsilon/2+\beta/\xi-m^2/(4\xi^2)-F\xi/4]^{1/2} ,$$

between the inner and outer turning points $\xi_<$, $\xi_>$,

Within a semiclassical treatment the dipole matrix elements between the initial state $|g\rangle$ and the energy normalized eigenstates $|\varepsilon\beta m\rangle$ may be written in the form[13,16]

$$\langle \varepsilon\beta m|D|g\rangle = A^{-1}\left[\frac{1}{\pi}\frac{\partial w}{\partial\beta}\right]^{-1/2} D_{\varepsilon\beta m} , \tag{5}$$

with $D_{\varepsilon\beta m}$ representing dipole matrix elements between the initial state $|g\rangle$ and β-normalized energy eigenstates $|\overline{\varepsilon\beta m}\rangle$ of H_A, which for $0<\varepsilon\ll 1$ are normalized so that

$$\langle \mathbf{x}|\overline{\varepsilon\beta m}\rangle \sim N_{\varepsilon\beta m}(\xi\eta)^{|m|/2}\frac{e^{im\phi}}{\sqrt{2\pi}} \quad (|\mathbf{x}|\ll 1) \tag{6}$$

with

$$N_{\varepsilon\beta m}=\begin{cases}\sqrt{2}[\beta(1-\beta)]^{|m|/2}(|m|!)^{-2}\Theta(1-\beta)\Theta(\beta) & (m\neq 0)\\ \sqrt{2}(1+e^{-2\pi\beta/k})^{-1/2}(1+e^{-2\pi(1-\beta)/k})^{-1/2} & (m=0)\end{cases}$$

and $k=\sqrt{2\varepsilon}$. $\Theta(x)$ is the unit step function with $\Theta(x)=1$ for $x>0$. Thereby, the factors $(1+e^{-2\pi\beta/k})^{-1/2}$ and $(1+e^{-2\pi(1-\beta)/k})^{-1/2}$ approximately take into account effects due to the Coulomb barriers, which are formed in the cases of $\beta<0$ or $\beta>1$ (see Fig. 1) and which are most important for $m=0$ states, due to the lack of the angular momentum barrier.[13]

Since the dipole matrix elements $D_{\varepsilon\beta m}$ get their dominant contribution from a region of the size of the initially occupied low-lying bound state $|g\rangle$, Eq. (6) shows that $D_{\varepsilon\beta m}$ is approximately independent of ε and F as long as $|\varepsilon|, F\ll 1$. As has been shown by Fano[15] and Harmin[16] and as outlined in the Appendix, these matrix elements may be related to spherical hydrogenic dipole matrix elements $\langle \varepsilon lm|D|g\rangle$.

The quantities A^{-1} and $[(1/\pi)(\partial w/\partial\beta)]^{-1/2}$ contain information about the motion of the excited electron in the ξ and η coordinate at large distances from the nucleus, where the static electric field is comparable to or larger than the Coulomb field due to the ionic core. The quantity

$$A^{-2}=\sum_{N=0}^{\infty} e^{2iN[w(\eta_1,\eta_2)-\pi/2+\delta]}R^N + \sum_{N=1}^{\infty} e^{-2iN[w(\eta_1,\eta_2)-\pi/2+\delta]}R^N \tag{7}$$

describes all effects due to the potential barrier associated with the motion in the η coordinate.[16] For energies below this potential barrier, $w(\eta_1,\eta_2)$ is the classical action between the inner and outer turning points of the potential well and

$$R=(1+e^{-2w(\eta_2,\eta_3)})^{-1/2}$$

is the reflection coefficient of the barrier, which involves the tunnel integral $w(\eta_2,\eta_3)$. δ is an additional phase shift due to the potential barrier, which tends to zero far above or below the top of the barrier. Above the top of the potential barrier, $w(\eta_2,\eta_3)<0$ and R rapidly tends to zero.[20] In particular, for energies above the zero-field photoionization threshold ($\varepsilon>0$), we may therefore neglect effects due to reflection above the potential barrier and approximately have $A^{-2}\approx 1$.

With the help of the Poisson summation formula,[21] the sum over the quantum number n_1 in Eq. (2) can be converted to a sum over integrals involving factors of the form $e^{i2Mw(\varepsilon,\beta,m)}$. The corresponding energy integrals can then be performed with the help of contour integration in the complex-ε plane, thereby using the fact that for $|\varepsilon|\to\infty$ we have $e^{iw(\varepsilon,\beta m)}\to 0$ in the upper half of the complex-ε plane. Setting $A=1$ and using Eqs. (5) and (A5) we thus obtain, in the case $0<\varepsilon\ll 1$, for the self-energy the expression

$$\Sigma(\varepsilon)=\Sigma^{(s)}-2\pi i\sum_{M=1}^{\infty}\sum_{m}\int_{\beta^0}^{\infty} d\beta\, e^{2iM[w(\varepsilon,\beta,m)-\pi/2]}\times|D_{\varepsilon\beta m}|^2 , \tag{8}$$

with $\beta^0=\beta(n_1=0,\varepsilon,m)$ and

$$\Sigma^{(s)}=\delta\omega-i\Gamma/2 .$$

The laser-induced quadratic Stark shift of state $|g\rangle$, $\delta\omega$, due to the laser field and the ionization rate

$$\Gamma=2\pi\sum_{l,m}|\langle \varepsilon lm|D|g\rangle|^2$$

are independent of ε and F and characterize one-photon ionization from the initial state $|g\rangle$ in the absence of a static electric field. The residual terms in Eq. (8) may be attributed to repeated returns of the excited electron to the reaction zone, where the atom-laser interaction is localized and the dipole matrix elements $D_{\varepsilon\beta m}$ get their dominant contribution. With the mth return to the reaction zone, the wave function of the excited electron has accumulated a phase $2M[w(\varepsilon,\beta,m)-\pi/2]$, which is determined by the classical action associated with the motion in the ξ coordinate $w(\varepsilon,\beta,m)$ and the additional phase shifts of $\pi/2$, due to reflection at the classical turning points. [With each turning point there is associated a Morse index of 1 (Ref. 22).] $e^{2iw(\varepsilon,\beta,m)M}$ is a rapidly oscillating function of β with monotonically increasing phase. Furthermore, according to Eq. (6) the dipole matrix elements $D_{\varepsilon\beta m}$ rapidly tend to zero as a function of β outside the interval (0,1). As long as $\partial w/\partial\beta\gg 1$, the dominant contributions to these integrals come from small regions around the end points $\beta=0,1$ with the contribution at $\beta=0$ negligible, since, for $\varepsilon>0$, $\partial w/\partial\beta$ tends to infinity at $\beta=0$. Evaluating the β integrals asymptotically with the help of partial integration,[23] we thus find

$$\Sigma(\varepsilon)=\Sigma^{(s)}-\pi\delta_{m,0}\sum_{M=1}^{\infty}e^{2iM[w(\varepsilon,\beta,m)-\pi/2]}\{\sinh[M\lambda(\varepsilon)]\}^{-1}|D^{0}_{\varepsilon\beta m}|^{2}\sqrt{2\varepsilon}|_{\beta=1}\ , \tag{9}$$

with the dipole interaction matrix element

$$D^{0}_{\varepsilon\beta=1m=0}=\sum_{l=0}^{\infty}(-1)^{l}\sqrt{2l+1}\langle\varepsilon lm=0|D|g\rangle$$

between the initially occupied state $|g\rangle$ and a hydrogenic energy eigenstate, which describes asymptotically an electron moving in the direction of the applied electric field

The asymptotic expression (9) demonstrates the fact that only electrons, which leave the atom in the direction of the static electric field, i.e., with $\alpha=0$ or equivalently $\beta=1$, are able to return again to the reaction zone and thus contribute to the self-energy. Such an electron emission can only take place, if the excited electron hydrogenic states have a zero-angular-momentum component in the direction of the electric field. Otherwise, the probability of finding the excited electron along the electric field axis is negligibly small.

For $\varepsilon>0$ the modification of the self-energy due to the static electric field is completely determined by quantities characterizing the classical periodic motion of the excited electron in the direction of the electric field, namely, the classical action

$$w(\varepsilon,\beta=1,m=0)=F^{-1/2}B^{-1/2}[\tfrac{2}{3}CK(\kappa)+\tfrac{2}{3}\varepsilon BE(\kappa)] \tag{10}$$

with

$$B=2(\varepsilon^{2}+4F)^{1/2}/F\ ,$$

$$C=[(\varepsilon^{2}+4F)^{1/2}/F][(\varepsilon^{2}+4F)^{1/2}-\varepsilon]\ ,$$

$$\kappa=[(\varepsilon^{2}+4F)^{1/2}+\varepsilon]/[2(\varepsilon^{2}+4F)^{1/2}]\ ,$$

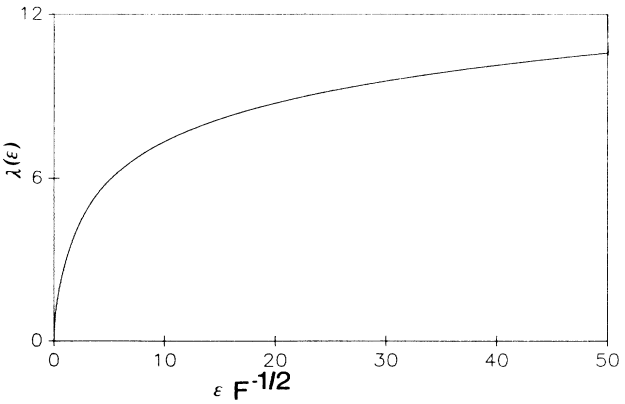

FIG. 2. Lyapunov exponent of the isolated classical periodic orbit.

and the Lyapunov exponent

$$\lambda(\varepsilon)=\sqrt{2\varepsilon}\frac{\partial w}{\partial\beta}\bigg|_{\beta=1}=\sqrt{2\varepsilon}2B^{-1/2}F^{-1/2}K(\kappa) \tag{11}$$

of the isolated periodic orbit. $K(\kappa)$ and $E(\kappa)$ are complete elliptic integrals of the first and second kind as defined in Ref. 24. Figure 2 shows the Lyapunov exponent, which only depends on the scaled variable $\varepsilon/\sqrt{F}$. Whereas the classical trajectory is stable at $\varepsilon=0$, i.e., $\lambda(\varepsilon=0)=0$, it becomes unstable for $\varepsilon>0$ with a monotonically increasing Lyapunov exponent $\lambda(\varepsilon)$. For $\varepsilon/\sqrt{F}\ll1$, this Lyapunov exponent has recently also been evaluated by Wintgen by numerical integration of the classical equations of motion.[18]

According to Eq. (9) in the limit $F\ll1$ the dominant contributions to the self-energy $\Sigma(\varepsilon)$ are of the order of $O(F^{1/4})$. Any modifications of this result due to the linear Stark effect of the initial atomic state $|g\rangle$ give rise to corrections, which are at most of the order of $O(F)$, and are therefore negligible in the limit $F\ll1$.

III. RESULTS AND DISCUSSION

In this section we calculate the time evolution of the initial-state probability amplitude $a_g(t)$ on the basis of Eqs. (1) and (8) for the case of laser excitation of continuum states slightly above the zero-field photoionization threshold, i.e., $0<\varepsilon\ll1$. With the help of a multiple scattering representation of $a_g(t)$, we derive an asymptotic expression valid in the limit $F\ll1$, which explicitly shows how the classical properties of the periodic motion of the excited electron in the direction of the applied electric field manifest themselves in the dynamics of the laser-excitation process.

In order to obtain the time evolution of the initial-state probability amplitude $a_g(t)$, we have to invert the Laplace transform $a_g(z)$ as given in Eq. (1). Traditionally this is achieved with the help of contour integration in the complex z plane, which yields the initial-state-probability amplitude as a sum over contributions due to all dressed states of the strongly coupled atom-laser system. Here, however, it is much more convenient to express the initial-state-probability amplitude as a sum over contributions which may be attributed to the repeated returns of the excited electron to the reaction zone, where the atom-laser interaction is localized. This multiple-scattering expansion[2] is obtained from Eqs. (1) and (8) by rewriting them in the form

$$a_g(\varepsilon-\omega)=i(\varepsilon-\bar{\varepsilon}+i\Gamma/2)^{-1}+2\pi i(\varepsilon-\bar{\varepsilon}+i\Gamma/2)^{-1}\sum_{m_1,m_2}\int_{\beta_1^0}^{\infty}d\beta_1\int_{\beta_2^0}^{\infty}d\beta_2 D^*_{\varepsilon\beta_1 m_1}Y_{\beta_1 m_1\beta_2 m_2}$$
$$\times e^{2i[w(\varepsilon,\beta_2,m_2)-\pi/2]}D_{\varepsilon\beta_2 m_2}i(\varepsilon-\bar{\varepsilon}+i\Gamma/2)^{-1}\,, \tag{12}$$

with

$$Y_{\beta_1 m_1\beta_2 m_2}=-\delta(\beta_1-\beta_2)\delta_{m_1,m_2}+\sum_{m_3}\int_{\beta_3^0}^{\infty}d\beta_3 Y_{\beta_1 m_1\beta_3 m_3}e^{2i[w(\varepsilon,\beta_3,m_3)-\pi/2]}\chi_{\beta_3 m_3,\beta_2 m_2} \tag{13}$$

and the scattering matrix

$$\chi_{\beta_1 m_1,\beta_2 m_2}=\delta(\beta_1-\beta_2)\delta_{m_1,m_2}-2\pi i D_{\varepsilon\beta_1 m_1}(\varepsilon-\bar{\varepsilon}+i\Gamma/2)^{-1}D^*_{\varepsilon\beta_2 m_2}\,. \tag{14}$$

The second term of Eq. (14) thereby describes laser-assisted electron-ion scattering between the excited electronic channels (β_1,m_1) and (β_2,m_2) inside the reaction zone. $\bar{\varepsilon}=\varepsilon_g+\omega+\delta\omega$ is the mean excited energy. Inverting the Laplace transform we obtain from Eq. (12).

$$a_g(t)=e^{-i(\bar{\varepsilon}-\omega)t}e^{-\Gamma t/2}+\int_{-\infty}^{\infty}d\varepsilon\, e^{-i(\varepsilon-\omega)t}i(\varepsilon-\bar{\varepsilon}+i\Gamma/2)^{-1}$$
$$\times\sum_{m_1,m_2}\int_{\beta_1^0}^{\infty}d\beta_1\int_{\beta_2^0}^{\infty}d\beta_2 D^*_{\varepsilon\beta_1 m_1}Y_{\beta_1 m_1\beta_2 m_2}e^{2i[w(\varepsilon,\beta_2,m_2)-\pi/2]}D_{\epsilon\beta_2 m_2}i(\varepsilon-\bar{\varepsilon}+i\Gamma/2)^{-1}\,. \tag{15}$$

Solving Eq. (13) iteratively with the starting value

$$Y^0_{\beta_1 m_1\beta_2 m_2}=-\delta(\beta_1-\beta_2)\delta_{m_1,m_2}$$

and inserting the resulting series in Eq. (15), we obtain the multiple-scattering representation of the initial-state-probability amplitude.

As for the asymptotic expression for the self energy given in Eq. (9), the integrals over the separation parameter β in the multiple-scattering expansion can be performed by partial integration as long as $\partial w/\partial\beta\propto F^{-1/4}\gg 1$ [see Eq. (11)]. Then β values around $\beta=1$ dominate. Furthermore, if we are exciting an energy region above the zero-field photoionization threshold, which is sufficiently small in that $\partial^2 w/\partial\varepsilon^2|_{\beta=1}\Gamma^2\ll 1$ we may approximate the energy integration in Eq. (15) by linearizing the phase of the exponential functions to obtain

$$a_g(t)=e^{-i(\bar{\varepsilon}-\omega)t}e^{-\Gamma t/2}+e^{-i(\bar{\varepsilon}-\omega)t}2\pi i\delta_{m,0}|D^0_{\bar{\varepsilon}\beta m}|^2(\sqrt{2\bar{\varepsilon}}/\Gamma)\{\sinh[\lambda(\bar{\varepsilon})]\}^{-1}e^{2i[w(\bar{\varepsilon},\beta,m)-\pi/2]}x_1e^{-x_1}\Theta(x_1)|_{\beta=1}$$
$$+e^{-i(\bar{\varepsilon}-\omega)t}2\pi i\delta_{m,0}|D^0_{\bar{\varepsilon}\beta m}|^2(\sqrt{2\bar{\varepsilon}}/\Gamma)e^{4i[w(\bar{\varepsilon},\beta,m)-\pi/2]}$$
$$\times\{\sinh[2\lambda(\bar{\varepsilon})]\}^{-1}x_2e^{-x_2}\Theta(x_2)|_{\beta=1}+2\pi i|D^0_{\bar{\varepsilon}\beta m}|^2(\sqrt{2\bar{\varepsilon}}/\Gamma)\{\sinh[\lambda(\bar{\varepsilon})]\}^{-2}\tfrac{1}{2}x_2^2e^{-x_2}\Theta(x_2)|_{\beta=1}+\cdots \tag{16}$$

with $x_M=(\Gamma/2)(t-MT_{\bar{\varepsilon}})$ and the classical orbit time of the excited electron $T_\varepsilon=2\partial w/\partial\varepsilon|_{\beta=1}$.

Equation (16) shows that as soon as the exciting laser pulse becomes so intense that the depletion time of the initial state $1/\Gamma$ is short in comparison with the classical orbit time of the excited electron $T_{\bar{\varepsilon}}$, the various contributions to the initial-state-probability amplitude are well separated in time. Then the laser-excitation process is not only localized in space by the finite size of the reaction zone but also in time so as to generate a radially localized electronic wave packet.[2] This wave packet leaves the reaction zone in a time of the order of $1/\Gamma$, corresponding to the exponential decay of the initial-state-probability amplitude evident from the first term of Eq. (16). In the energy region slightly above the zero-field photoionization threshold, which we are studying here, only a small fraction of the excited electronic wave packet is able to return later to the reaction zone. This returning part is due to electron emission within a small angular region around the direction of the applied static electric field, which corresponds to a small range of β values of the order of $\Delta\beta\approx(\partial w/\partial\beta)^{-1}_{\beta=1}$ around $\beta=1$. The combined Coulomb field of the ionic core and the applied static electric field cause the residual part of the wave packet to leave the atomic core without returning. At time $t\approx T_{\bar{\varepsilon}}$ the returning part of the generated wave packet reenters the reaction zone, where the atom-laser interaction is localized. There the electron may recombine with the ionic core, increasing the initial-state probability as evident from the second term of Eq. (16). Alternatively, the returning part may also leave the ionic core region again with part of it scattered in all directions by the action of the laser field inside the reaction zone. This laser-assisted electron-ion scattering process is character-

ized by the second term of the scattering matrix $\chi_{\beta_1 m_1,\beta_2 m_2}$ of Eq. (14). The part of the wave packet which returns again to the reaction zone at $t \approx 2T_{\bar{\varepsilon}}$ consists of two contributions: one originates from the unscattered part and is described by the third term of Eq. (16) and the other one is due to the scattered part and is represented by the fourth term. As long as $(\partial w/\partial\beta)_{\beta=1} \gg 1$, the contribution due to the scattered part is negligible in comparison with the unscattered part so that laser-assisted electron-ion scattering inside the reaction zone may be neglected. Physically this occurs because the periodic motion of the excited electron in the direction of the static electric field with $\alpha=0$ is represented by an isolated and unstable classical trajectory. Electron emission at slightly different angles $\alpha \neq 0$, which, e.g., is due to any scattering process inside the reaction zone, no longer leads to a periodic motion and therefore cannot manifest itself in the initial-state-probability amplitude. Neglecting laser-assisted electron-ion scattering inside the reaction zone, we thus finally find from Eq. (16)

$$a_g(t)=e^{-i(\bar{\varepsilon}-\omega)t}e^{-\Gamma t/2}+e^{-i(\bar{\varepsilon}-\omega)t}2\pi i\delta_{m,0}|D^0_{\bar{\varepsilon}\beta m}|^2(\sqrt{2\bar{\varepsilon}}/\Gamma)\sum_{M=1}^{\infty}\{\sinh[M\lambda(\bar{\varepsilon})]\}^{-1}e^{2iM[w(\bar{\varepsilon},\beta,m)-\pi/2]}x_M e^{-x_M}\Theta(x_M)|_{\beta=1}\,. \tag{17}$$

The general expression for the multiple-scattering representation of $a_g(t)$ as given in Eq. (15) and the approximate relation of Eq. (17) are the main results of this paper.

Figure 3 shows the time evolution of the initial-state probability according to Eq. (17) in the case of laser excitation of hydrogenic states with $\bar{\varepsilon}=5\times10^{-5}$, $l=1$, $m=0$, and $F=10^{-8}$. The total ionization rate is $\Gamma=7\times10^{-6}$ so that $1/\Gamma < T_{\bar{\varepsilon}}$ and the laser-excitation process is localized in space and time. This implies the generation of an electronic wave packet. Typically, for $t < T_{\bar{\varepsilon}}$, $|a_g(t)|^2$ decays exponentially and for $t > T_{\bar{\varepsilon}}$, $|a_g(t)|^2$ increases at multiples of the classical orbit time because of stimulated recombination. However, due to the large instability of the excited periodic orbit, which is characterized by the Lyapunov exponent $\lambda(\varepsilon)$ of Eq. (11), the amplitudes of successive recombination peaks decrease rapidly.

According to Eq. (17) in the case of a laser pulse with T longer than $T_{\bar{\varepsilon}}$, the various contributions associated with different returns of the excited electron to the reaction zone overlap in time so that the initial-state probability reflects the quantum-mechanical interference between the corresponding probability amplitudes. An extreme situation arises in the case of excitation by a long and weak laser pulse with $T_{\bar{\varepsilon}} \ll T \ll 1/\Gamma$. Then essentially all terms of Eq. (17) contribute to $|a_g(T)|^2$ and the laser-excitation process can be described by a time-independent rate

$$R=\frac{d}{dT}(1-|a_g(T)|^2)=\Gamma\left[1+2\pi\delta_{m,0}|D^0_{\bar{\varepsilon}\beta m}|^2\frac{\sqrt{2\bar{\varepsilon}}}{\Gamma}\sum_{M=1}^{\infty}\frac{\sin\{2M[w(\bar{\varepsilon},\beta,m)-\pi/2]\}}{\sinh[M\lambda(\bar{\varepsilon})]}\right]_{\beta=1}, \tag{18}$$

which in general is related to the imaginary part of the self energy of Eq. (2) by

$$R=-2\,\mathrm{Im}[\Sigma(\bar{\varepsilon})]=2\pi\sum_m\sum_{n_1=0}|\langle\bar{\varepsilon}\beta m|D|g\rangle|^2\,. \tag{19}$$

An expression equivalent to Eq. (18) has been derived by Bogomolny[25] for the time-independent rate describing laser excitation by a weak and long pulse.

Figure 4 compares the energy dependence of the asymptotic excitation rate R of Eq. (18) (dashed line) with the exact rate of Eq. (19) (solid line). In Eq. (19) the required parabolic dipole matrix elements have been evaluated with the help of Eqs. (5), (6), (A3), and (A4). The deviations of the result of Eq. (18) from the exact Eq. (19) occur because at a field strength of $F=10^{-6}$ the asymptotic parameter $(\partial w/\partial\beta)_{\beta=1} \propto F^{-1/4}$ is still not

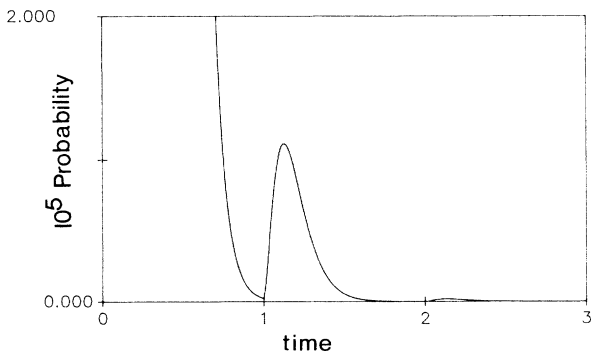

FIG. 3. Initial-state probability $|a_g(t)|^2$ as a function of time (in units of the classical orbit time $T_{\bar{\varepsilon}}$) for $F=10^{-8}$, $\bar{\varepsilon}=5\times10^{-5}$, $\Gamma=7\times10^{-6}$ a.u.

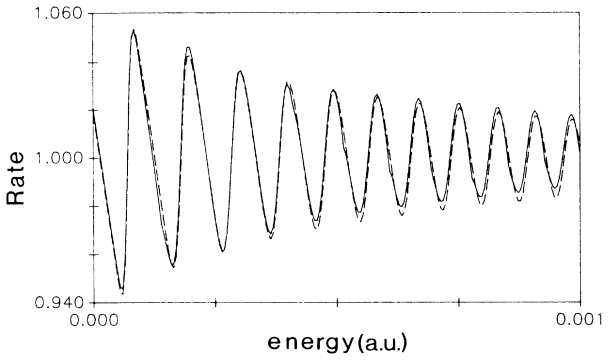

FIG. 4. Energy dependence of the asymptotic excitation rate R/Γ of Eq. (19) (solid line) and of the corresponding asymptotic expression of Eq. (18) (dashed line) for $F=10^{-6}$ a.u.

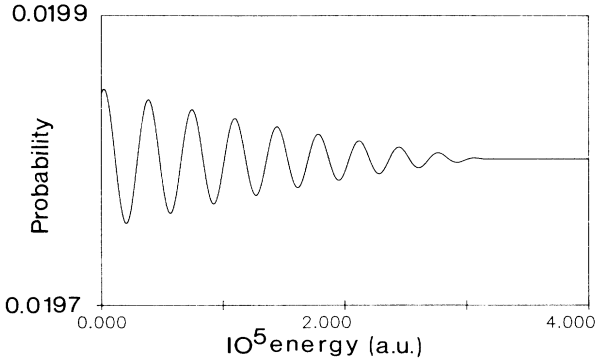

FIG. 6. Initial-state probability $|a_g(T)|^2$ as a function of the mean excited energy for $F=10^{-8}$, $T=2\times10^6$ ($T_{\bar{\varepsilon}=0}=1.7\times10^6$) a.u.

sufficiently large to allow asymptotic evaluation of the β integrals in Eq. (15).

Figure 5 shows the energy dependence of the excitation rate R for $F=10^{-8}$ (solid line). For this value of the field strength the results of Eqs. (18) and (19) are indistinguishable. Close to the zero-field photoionization threshold, the periodic orbit is relatively stable, i.e., $\lambda(\bar{\varepsilon})\ll 1$. The line shape of the excitation rate resembles a characteristic saw-tooth,[13,26] which corresponds to the limit $\bar{\varepsilon}\to 0$ in Eq. (18) and is shown by the dashed line in Fig. 5. With increasing values of $\bar{\varepsilon}$, the periodic orbit eventually becomes sufficiently unstable so that $\lambda(\bar{\varepsilon})>1$ and the line shape becomes more and more sinusoidal as the number of significant terms in Eq. (18) becomes smaller and smaller.

Figure 6 shows the initial-state probability $|a_g(T)|^2$ as a function of the mean excited energy for a weak and short laser pulse with $1/\Gamma \gg 2T_{\bar{\varepsilon}=0} > T > T_{\bar{\varepsilon}=0}$. According to Eq. (17) then, only the contribution associated with the first return of the excited electron to the reaction zone contributes to $|a_g(T)|^2$ for sufficiently small values of $\bar{\varepsilon}$. With increasing values of the mean excited energy $\bar{\varepsilon}$, the classical orbit time $T_{\bar{\varepsilon}}$ eventually becomes larger than the pulse duration T and the excited electron is no longer able to return to the reaction zone during the interaction with the laser pulse. In this case, the laser-excitation process is localized in space and time and an electronic wave packet is generated. As a consequence, the initial-state probability is completely determined by the direct ionization process, which takes place before the excited wave packet has left the reaction zone, and becomes independent of $\bar{\varepsilon}$.

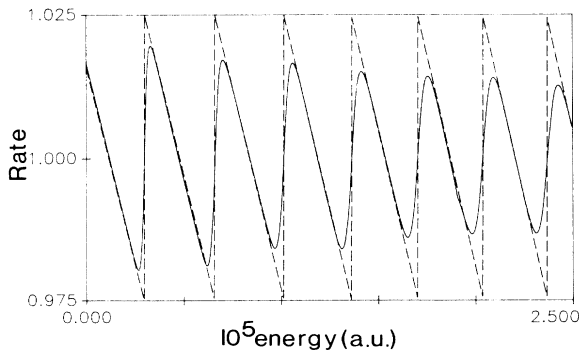

FIG. 5. Energy dependence of the asymptotic excitation rate R/Γ of Eq. (18) (solid line) and of the limiting saw-tooth-like line shape (dashed line) for $F=10^{-8}$ a.u.

IV. CONCLUSION

We have studied one-photon excitation of hydrogen in the presence of a static electric field in the energy region slightly above the zero-field photoionization threshold. It has been shown that, in the case of laser polarization parallel to the applied static electric field, excitation by an intense or short laser pulse leads to the generation of an electronic wave packet, part of which performs a periodic motion which is controlled by the external electric field and the Coulomb field of the ionic core. With the help of a multiple-scattering representation, we have derived an analytical expression for the time dependence of the initial-state-probability amplitude, which is asymptotically valid in the limit of a weak static electric field, i.e., $F\ll 1$. This expression shows how the characteristics of the corresponding classical periodic orbit manifest themselves in the dynamics of the laser-excitation process.

In the case of excitation by an intense laser pulse, we have shown that with each return to the reaction zone, where the atom-laser interaction is localized, the generated electronic wave packet may recombine with the ionic core to increase the initial-state probability. The height of the recombination peaks reveals how unstable the excited periodic orbit is. We have also studied laser excitation by pulses weak in the sense that the depletion time of the initially occupied bound state is larger than the classical orbit time of the excited electron. As long as the classical orbit time of the excited electron is small in comparison with the pulse duration, the frequency dependence of the excitation probability shows the characteristic behavior, which has been found previously, namely, a change

from a saw-tooth shape close to threshold to a sinusoidal shape sufficiently far above threshold. However, smaller pulse durations may change this type of behavior.

ACKNOWLEDGMENTS

This work was supported by the Austrian "Fonds zu Foerderung der wissenschaftlichen Forschung" under Contract No. P6008P. Stimulating discussions with P. Zoller and D. Wintgen are gratefully acknowledged.

APPENDIX

In this Appendix we summarize some relations between hydrogenic energy eigenstates in parabolic and spherical coordinates, which are used in Sec. II.

The energy normalized parabolic eigenstates $|\varepsilon\beta m\rangle_{\rm H}$ of hydrogen are related to the corresponding spherical energy eigenstates $|\varepsilon lm\rangle$ by[19]

$$|\varepsilon\beta m\rangle_{\rm H}=\sum_{l=|m|}^{\infty}\langle lm|j\mu_+,j\mu_-\rangle|\varepsilon lm\rangle\ , \tag{A1}$$

with the Wigner coefficients $\langle lm|j\mu_+,j\mu_-\rangle$. In particular, for $\varepsilon<0$ we have $j=(\nu-1)/2$, $\mu_\pm=(m\pm\nu A_z)/2$, and $\nu=(-2\varepsilon)^{-1/2}$. For $\varepsilon>0$ the angular momentum j and its component $\mu_\pm$ become complex. Following Fano[15] and Harmin[16] this relation may be rewritten in the form

$$|\varepsilon\beta m\rangle_{\rm H}=\sum_{l=|m|}^{\infty}a_{\beta l}^{\varepsilon m}\frac{N_{\varepsilon\beta m}^{\rm H}}{N_{\varepsilon lm}}|\varepsilon lm\rangle\ , \tag{A2}$$

with

$$\langle\mathbf{x}|\varepsilon lm\rangle\sim N_{\varepsilon lm}r^l Y_l^m(\theta,\phi)\ ,$$

$$\langle\mathbf{x}|\varepsilon\beta m\rangle_{\rm H}\sim N_{\varepsilon\beta m}^{\rm H}(\xi\eta)^{|m|/2}\frac{e^{im\phi}}{\sqrt{2\pi}}\quad(|\mathbf{x}|\ll 1)\ .$$

The coefficients $a_{\beta l}^{\varepsilon m}$ now characterize the pure geometrical aspect of the transformation between parabolic and spherical coordinates and are independent of the normalization of the wave functions.

Inside the Coulomb zone, which is characterized by $r\ll F^{-1/2}$,[16] where the external electric field is negligible in comparison with the Coulomb potential, the energy eigenstates $|\overline{\varepsilon\beta m}\rangle$ of H_A can be related to spherical hydrogenic energy eigenstates $|\varepsilon lm\rangle$ by

$$\langle\mathbf{x}|\overline{\varepsilon\beta m}\rangle=\sum_{l=|m|}^{\infty}a_{\beta l}^{\varepsilon m}\frac{N_{\varepsilon\beta m}}{N_{\varepsilon lm}}\langle\mathbf{x}|\varepsilon lm\rangle\quad(|\mathbf{x}|\ll F^{-1/2}) \tag{A3}$$

with $N_{\varepsilon lm}=2^{l+1}/(2l+1)!$. Since the dipole matrix elements $\langle\overline{\varepsilon\beta m}|D|g\rangle$ are dominated by this spatial region, the same relation holds between $\langle\overline{\varepsilon\beta m}|D|g\rangle$ and the spherical dipole matrix elements $\langle\varepsilon lm|D|g\rangle$. An explicit expression for the coefficients $a_{\beta l}^{\varepsilon m}$ is given in Ref. 16 which reduces in the limit β, $(1-\beta)\gg l\sqrt{2\varepsilon}$ to

$$a_{\beta l}^{\varepsilon m}=(-1)^{|m|}\sqrt{4l+2}(|m|!)^2[(2l+1)!!]^{-1}[(l+m)!(l-m)!]^{-1/2}\sum_{k=0}^{l-|m|}(-1)^k\begin{bmatrix}l-|m|\\k\end{bmatrix}\begin{bmatrix}l+|m|\\l-k\end{bmatrix}\beta^k(1-\beta)^{l-|m|-k}\ . \tag{A4}$$

Using Eq. (A4) together with the relation for $N_{\varepsilon\beta m}$ as given in Eq. (6), we find

$$\int_{\beta^0}^{\infty}d\beta|D_{\varepsilon\beta m}|^2=\sum_{l=|m|}^{\infty}|\langle\varepsilon lm|D|g\rangle|^2 \tag{A5}$$

as long as $\beta^0=\beta(n_1=0,\varepsilon,m)<0$.

*Present address: Fakultät für Physik, Albert-Ludwigs-Universität, Herman-Herder-Strasse 3, D-7800 Freiburg, West Germany.

[1]G. Alber, H. Ritsch, and P. Zoller, Phys. Rev. A **34**, 1058 (1986).
[2]G. Alber and P. Zoller, Phys. Rev. A **37**, 377 (1988).
[3]G. Alber, Th. Haslwanter, and P. Zoller, J. Opt. Soc. Am. B **5**, 2439 (1988).
[4]A. Giusti and P. Zoller, Phys. Rev. A **36**, 5178 (1987).
[5]D. Kleppner, M. G. Littman, and M. L. Zimmerman, in *Rydberg States of Atoms and Molecules,* edited by R. F. Stebbings and F. B. Dunning (Cambridge, New York, 1983), p. 73.
[6]P. F. O'Mahony, in *Fundamental Processes of Atomic Dynamics,* edited by J. S. Briggs, H. Kleinpoppen, and H. O. Lutz (Plenum, New York, 1987) p. 197.
[7]H. A. Bethe and E. E. Salpeter, *Quantum Mechanics of One- and Two-Electron Atoms* (Plenum, New York, 1977).
[8]R. R. Freeman and N. P. Economu, Phys. Rev. A **20**, 2356 (1979).
[9]S. Feneuille, S. Liberman, J. Pinard, and A. Taleb, Phys. Rev. Lett. **42**, 1404 (1979).
[10]W. L. Glab and M. H. Nayfeh, Phys. Rev. A **31**, 530 (1985).
[11]H. Rottke and K. H. Welge, Phys. Rev. A **33**, 301 (1986).
[12]A. R. P. Rau, J. Phys. B **12**, L193 (1979).
[13]V. D. Kondratovich and V. N. Ostrovsky, J. Phys. B **17**, 1981 **17**, 2011 (1984).
[14]E. Luc-Koenig and A. Bachelier, J. Phys. B **13**, 1743 (1980); **13**, 1769 (1980).

[15]U. Fano, Phys. A **24**, 619 (1981).
[16]D. A. Harmin, Phys. Rev. A **24**, 2491 (1981); **26**, 2656 (1982).
[17]W. P. Reinhardt, J. Phys. B **16**, L635 (1983).
[18]D. Wintgen, J. Phys. B **22**, L5 (1989).
[19]L. D. Landau and E. M. Lifschitz, *Quantum Mechanics,* 3rd ed. (Pergamon, Oxford, 1977).
[20]M. V. Berry and K. E. Mount, Rep. Prog. Phys. **35**, 315 (1972).
[21]P. M. Morse and H. Feshbach, *Methods of Theoretical Physics* (McGraw-Hill, New York, 1953).
[22]V. P. Maslov and M. V. Fedorink, *Semiclassical Approximation in Quantum Mechanics* (Reidel, Boston, 1981).
[23]C. M. Bender and S. A. Orszag, *Advanced Mathematical Methods for Scientists and Engineers* (McGraw-Hill, New York, 1978).
[24]*Handbook of Mathematical Functions,* Natl. Bur. Stand. Appl. Math. Ser. No. 55, edited by M. Abramowitz and I. Stegun (U.S. GPO, Washington, D.C., 1964).
[25]E. B. Bogomolny, Pis'ma Zh. Eksp. Teor. Fiz. **47**, 445 (1988) [JETP Lett. **47**, 526 (1988)].
[26]A. G. Aronov and A. S. Ioselevich, Zh. Eksp. Teor. Fiz. **74**, 1043 (1978) [Sov. Phys.—JETP **47**, 548 (1978)].